Abandoning Sverdrup's Critical Depth Hypothesis on phytoplankton blooms

Michael J. Behrenfeld[1]

Department of Botany and Plant Pathology, Cordley Hall 2082, Oregon State University, Corvallis, Oregon 97331-2902 USA

Abstract. The Critical Depth Hypothesis formalized by Sverdrup in 1953 posits that vernal phytoplankton blooms occur when surface mixing shoals to a depth shallower than a critical depth horizon defining the point where phytoplankton growth exceeds losses. This hypothesis has since served as a cornerstone in plankton ecology and reflects the very common assumption that blooms are caused by enhanced growth rates in response to improved light, temperature, and stratification conditions, not simply correlated with them. Here, a nine-year satellite record of phytoplankton biomass in the subarctic Atlantic is used to reevaluate seasonal plankton dynamics. Results show that (1) bloom initiation occurs in the winter when mixed layer depths are maximum, not in the spring, (2) coupling between phytoplankton growth (μ) and losses increases during spring stratification, rather than decreases, (3) maxima in net population growth rates (*r*) are as likely to occur in midwinter as in spring, and (4) *r* is generally inversely related to μ. These results are incompatible with the Critical Depth Hypothesis as a functional framework for understanding bloom dynamics. In its place, a "Dilution–Recoupling Hypothesis" is described that focuses on the balance between phytoplankton growth and grazing, and the seasonally varying physical processes influencing this balance. This revised view derives from fundamental concepts applied during field dilution experiments, builds upon earlier modeling results, and is compatible with observed phytoplankton blooms in the absence of spring mixed layer shoaling.

Key words: Critical Depth Hypothesis; grazing; growth rates; North Atlantic; phytoplankton blooms; remote sensing.

Introduction

The vernal, or spring, bloom is a renowned feature of many seasonal seas in the global ocean. Perhaps most famous of all is the annual greening event, clearly detectable from space (Fig. 1A), that occurs at middle and high latitudes of the North Atlantic. The physical–biological interactions responsible for this phenomenon have been studied since the 19th century (Banse 1992) and this interest continues unabated today. The emergence of plankton-rich waters in spring and early summer from the clear waters of winter, when light is low and storms frequent, naturally leads to the conclusion that the North Atlantic bloom is a consequence of improved upper ocean growth conditions in the spring that stimulate phytoplankton growth (analogous to spring growth of terrestrial vegetation in temperate ecosystems, where increased cell division drives biomass accumulation). This relationship between growth conditions and phytoplankton biomass was encapsulated in 1935 by Gran and Braarud in the concept of a "critical depth," which was later formalized by Sverdrup (1953) into the familiar "Critical Depth Hypothesis."

The fundamental tenet of the critical depth concept is that there exists, for any given date and location in the ocean, a surface mixing depth at which phytoplankton growth is precisely matched by losses of phytoplankton biomass within this depth interval. In Sverdrup's hypothesis, the vernal bloom is initiated when the surface mixed layer shoals to a depth less than the critical depth, allowing the bulk phytoplankton specific growth rate (μ) to exceed the bulk specific loss rate (*l*) such that net population growth (*r*) is possible:

$$r = \mu - l > 0. \qquad (1)$$

Importantly, Sverdrup assumed that *l* was a constant over time and thus independent of μ. Accordingly, he envisioned the vernal bloom as resulting from, not simply being correlated with, an increase in phytoplankton growth rates. This view remains prevalent today, but will be challenged herein. While often misinterpreted, Sverdrup's loss rate included sinking export, predator consumption (i.e., grazing), and respiration by the phytoplankton themselves, despite his use of the term "respiration" for *l* (Smetacek and Passow 1990). In more contemporary treatments (e.g., Crumpton and Wetzel 1982, Evans and Parslow 1985, Platt et al. 1991, Banse 1994), it is common practice to separate *l* into its component terms, such as

$$r = \mu - g - s - p - f \qquad (2)$$

where g is mortality due to grazing, s is losses due to sinking, p is losses due to viral infection and parasitism, and f includes physical flushing losses, including dilution by vertical mixing (Crumpton and Wetzel 1982, Banse 1994).

Sverdrup evaluated the Critical Depth Hypothesis by comparing temporal changes in phytoplankton abundance observed in 1949 at Weather Ship "M" (66° N, 2° E) to coincident changes in mixing depth relative to the critical depth horizon. He concluded that the observations were consistent with the hypothesis, but not without some astute (and often overlooked) caveats. First, Sverdrup noted that the "bloom" in phytoplankton biomass observed two days after "the depth of the mixed layer was for the first time smaller than the critical depth" (Sverdrup 1953:249) likely reflected the advection of high biomass waters into the Weather Ship "M" site, rather than rapid growth of the local phytoplankton population in response to the changed relationship between mixing depth and critical depth. He also recognized that, in the presence of grazers, the "phytoplankton population may remain small in spite of heavy production"; in other words, bloom formation is critically dependent on the relationship between phytoplankton growth and grazing. Finally and importantly, Sverdrup noted that, even in his spring 1949 data set, the first increase in phytoplankton biomass occurred prior to vertical stratification of the upper water column. With these issues in mind, Sverdrup concluded his classic paper with the following statement: "It is, therefore, not advisable to place too great emphasis on the agreement between theory and [the Weather Ship "M"] observations."

For over five decades, the Critical Depth Hypothesis has repeatedly reemerged in discussions of phytoplankton bloom dynamics and found its way into oceanographic and limnological textbooks. Nevertheless, criticisms have been raised (e.g., Smetacek and Passow 1990, Backhaus et al. 2003), with one reoccurring issue being the observation of significant spring phytoplankton blooms in the apparent absence of water column stratification (Heimdal 1974, Schei 1974, Townsend et al. 1992, Ellertsen 1993, Backhaus et al. 1999, Dale et al. 1999, Körtzinger et al. 2008). Here, I take a fresh look at seasonal phytoplankton cycles in the North Atlantic by using a synoptic tool unavailable to Sverdrup in 1953: satellite observations. With these data, it is clear that the Critical Depth Hypothesis is an inadequate framework for understanding vernal blooms. As a potential replacement, a "Dilution–Recoupling Hypothesis" is proposed that focuses on annual cycles in physical processes that alter the delicate balance between phytoplankton growth and losses.

The North Atlantic from Space

Seasonal cycles in North Atlantic phytoplankton were investigated using eight-day resolution remote sensing data from the Sea-viewing Wide Field-of-view Sensor (SeaWiFS) for the period January 1998 to December 2006. SeaWiFS-derived water leaving radiances emanate from the upper first optical depth of the water column (i.e., depth to which 10% of surface irradiance penetrates), thus phytoplankton features deeper in the water column are not detected. However, uniformity of phytoplankton properties within an active mixing layer implies that SeaWiFS products are generally representative of this layer, even during the deep winter mixing of the North Atlantic (Townsend et al. 1992, Ward and Waniek 2007, Boss et al. 2008; note, during midwinter, vertical velocities from convective mixing are still sufficient for mixed layer transit times of a few days or less [Backhaus et al. 2003, D'Asaro 2008]).

For the current study, satellite products used as indices of phytoplankton abundance were surface chlorophyll concentration (Chl$_{sat}$, mg/m^3; Fig. 1A) and phytoplankton carbon concentration (C_{phyt}, mg/m^3). Chl$_{sat}$ values were from the NASA standard OC4-V4 algorithm (the most familiar product to SeaWiFS users). For comparison, OC4-V4 Chl$_{sat}$ estimates are, on average, 29% higher than those from the Garver-Siegel-Maritorena (GSM) semi-analytical algorithm (Garver and Siegel 1997, Maritorena et al. 2002, Siegel et al. 2002b). Despite this bias, the two algorithms yield temporal patterns that are highly correlated ($r = 0.97$), so conclusions drawn here regarding phytoplankton seasonal cycles are insensitive to this choice of Chl$_{sat}$ product. Phytoplankton carbon concentrations were derived from GSM particulate backscattering coefficients (b_{bp}) following Behrenfeld et al. (2005).

The weakness of using Chl$_{sat}$ as an index of phytoplankton standing stock is that chlorophyll is also influenced by light- and nutrient-driven changes in intracellular pigment levels. The weakness of C_{phyt} is that it is derived from a scattering property that is not uniquely algal, so its relation to phytoplankton biomass is influenced by the stability of the particle size distribution. However, C_{phyt} is insensitive to physiological variability and appears to track phytoplankton biomass in the few studies conducted to date (Behrenfeld and Boss 2003, 2006, Behrenfeld et al. 2005, Siegel et al. 2005, Huot et al. 2007, Westberry et al. 2008, Dall'Olmo et al. 2009).

North Atlantic phytoplankton seasonal cycles were evaluated for 12 5° latitude × 10° longitude bins in the central open ocean basin and away from continental margins (Fig. 1A). The bins are roughly a factor of four larger than the high-latitude bins used by Banse and English (1994) and were chosen to minimize the influence of advection between eight-day periods, while maintaining a sense of spatial variability in phytoplankton seasonal properties. The lowest latitude bins (NA-1–NA-3) lie between 40° N and 45° N (Fig. 1A) and correspond to the "transitional region" discussed by Henson et al. (2008). For additional orientation, the 1989 North Atlantic Bloom Experiment (NABE) was located near the center of bin NA-4 (white star in Fig.
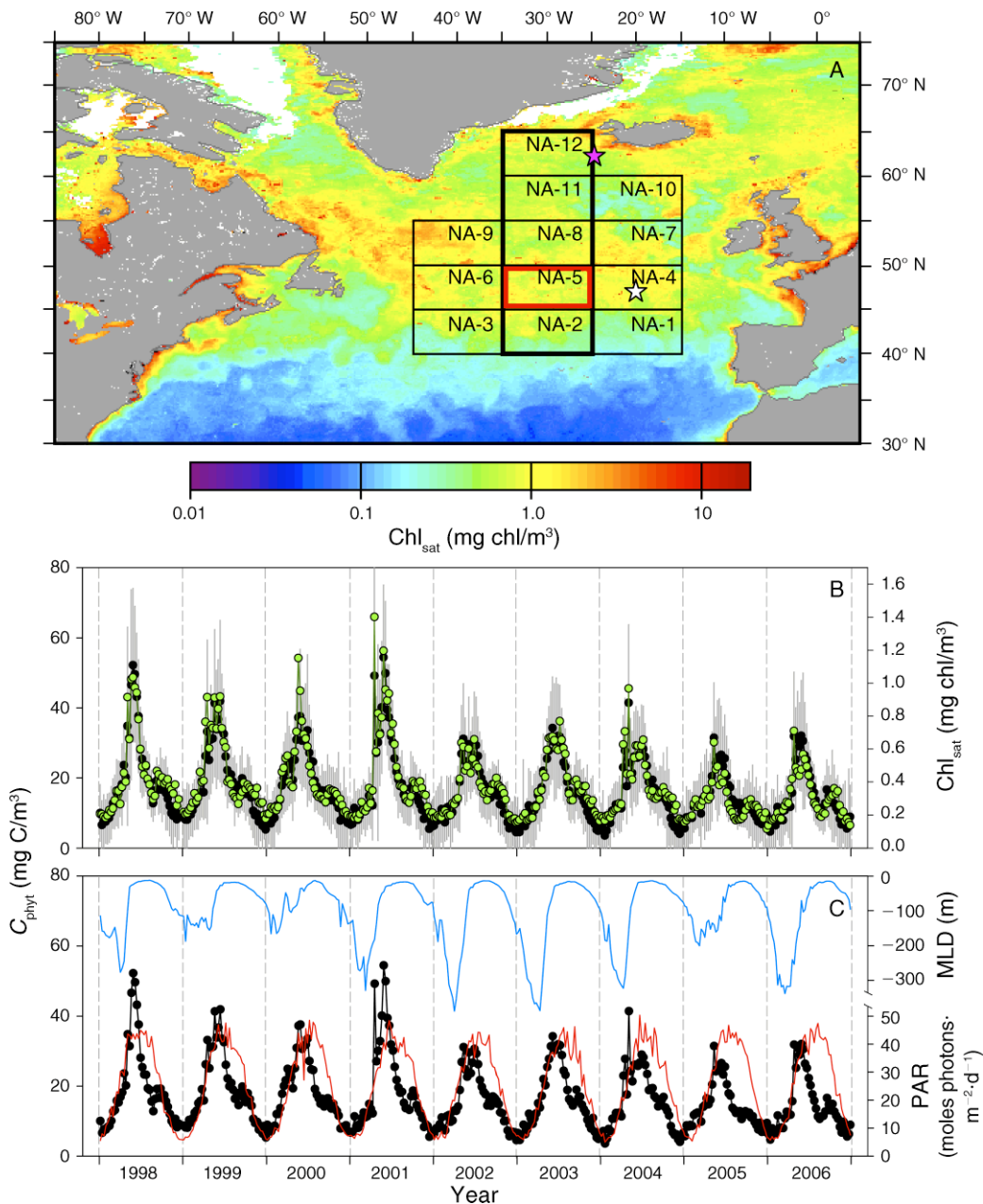
FIG. 1. (A) Typical late bloom surface chlorophyll concentrations (Chl_{sat}; note log scale) as observed from the satellite Sea-viewing Wide Field-of-view Sensor (SeaWiFS) in June 2002. Also shown are the 12 study bins and their designations. Red box: Figs. 1B, C, 2A, C, 3, and 4A–C show results from bin NA-5. Heavy black box: bins used in Fig. 2B–F. White star: 1989 North Atlantic Bloom Experiment (NABE) location. Pink star: 2008 North Atlantic Bloom (NAB) study location. (B) Nine-year record of phytoplankton biomass (C_{phyt}: black symbols, left axis) and Chl_{sat} (green symbols, right axis) at eight-day resolution for bin NA-5. Gray bars indicate within-bin standard deviations for C_{phyt}. (C) Nine-year record of C_{phyt} (black symbols, left axis, same as panel B), photosynthetically active radiation (PAR: red line, lower right axis), and mixed layer depth (MLD: blue line, upper right axis) for bin NA-5. Vertical dashed lines in panels B and C indicate 1 January of each year.

1A) and the recent North Atlantic Bloom (NAB) study (March–June 2008) coincides with the eastern edge of bin NA-12 (pink star in Fig. 1A). For the northernmost bins (NA-7–NA-12), satellite data were unavailable for a few weeks each year during midwinter. For all remaining times and locations, bin values represent means for all

observations within a given eight-day period, averaging >1200 cloud-free pixels per period (maximum potential = 1800 pixels). Less than 4% of the bin values were derived from <200 cloud-free pixels. Within-bin standard deviations for each eight-day mean value are shown for C_{phyt} in Fig. 1B.

Throughout the SeaWiFS record, regular Chl_{sat} and C_{phyt} seasonal cycles of variable amplitude (Henson et al. 2008) are found for each bin (Fig. 1B; see also the Appendix: Fig. A1 for all 12 bins). Spring chlorophyll peaks typically range from 0.5 to 2.0 mg/m^3, with occasional values exceeding 2.5 mg/m^3 (Fig. 1B; Appendix: Fig. A1). On average, peak concentrations of Chl_{sat} and C_{phyt} are lowest in the southern-most bins (Chl_{sat} = 0.72 ± 0.28 mg/m^3 [mean ± SD]; C_{phyt} = 33.9 ± 7.2 mg/m^3) and increase progressively to the north to reach values of Chl_{sat} = 1.18 ± 0.32 mg/m^3 and C_{phyt} = 81.9 ± 45.1 mg/m^3 in bins NA-10, NA-11, and NA-12. Timing of these seasonal peaks also changes with latitude, occurring roughly two weeks later with every 5° increase in latitude (Siegel et al. 2002a, Henson et al. 2008). Annual minima in Chl_{sat} and C_{phyt} are typically observed in January (Fig. 1B; Appendix: Fig. A1), with Chl_{sat} ranging from ~0.1 to 0.2 mg/m^3, in excellent agreement with field observations (Parsons and Lalli 1988, Banse 2002, Backhaus et al. 2003, Ward and Waniek 2007, Boss et al. 2008). During each seasonal cycle and in each bin, changes in Chl_{sat} and C_{phyt} are highly correlated (Fig. 1B; Appendix: Fig. A1; mean r = 0.84, range = 0.76–0.93), with the largest deviations observed during summer in the lowest latitude bins (NA-1–NA-3) and consistent with light-driven photo-acclimation responses to elevated mixed layer light levels (Behrenfeld et al. 2005, Siegel et al. 2005). The strong correspondence between Chl_{sat} and C_{phyt} reflects the large dynamic range in phytoplankton biomass in the North Atlantic overwhelming coincident physiological processes acting to distinguish these two properties. Accordingly, the same overall conclusions emerge regarding the North Atlantic bloom whether phytoplankton abundance is assessed using Chl_{sat} or C_{phyt}. For clarity, I have, therefore, restricted the remaining discussion and figures to seasonal cycles in C_{phyt}, but provide illustrations of seasonal Chl_{sat} cycles for each bin in the Appendix.

In Fig. 1C, the nine-year record of C_{phyt} for NA-5 (red box in Fig. 1A) is compared to coincident changes in mixed layer depth (MLD) and SeaWiFS cloudiness-corrected incident photosynthetically active radiation (PAR: 400–700 nm). Here, MLD values are from the Fleet Numerical Meteorology and Oceanography Center (FNMOC) model (Clancy and Sadler 1992) and the Simple Ocean Data Assimilation (SODA) model (available online).[2] Both are tuned to available in situ data (i.e., they are "data-assimilating models"). Perhaps the most striking features of Fig. 1C are that (1) winter through spring changes in phytoplankton biomass are highly correlated with changes in PAR, and (2) the largest changes in C_{phyt} coincide with spring MLD shoaling. Similar relationships are found for all 12 bins and may at first appear to confirm the Critical Depth

Hypothesis, but in fact they do not. The key problem is that correlation between phytoplankton standing stock (C_{phyt}), PAR, and MLD shoaling does not imply that a similar relationship exists for net growth rates (r). This is a crucial point because Sverdrup's Critical Depth Hypothesis is a statement that "shoaling of the mixed layer above the critical depth horizon initiates a spring bloom because it demarcates the first time when r becomes positive." To test this notion, one must therefore evaluate seasonal cycles in r. As demonstrated in the following sections, such an analysis tells a very different story about the North Atlantic bloom than that implied by Fig. 1C.

ABANDONING SVERDRUP

The net specific growth rate of a phytoplankton population can be calculated from two measures of biomass (C_0, C_1) separated by a period of time ($\Delta t = t_1 - t_0$) following

$$r = \ln(C_1/C_0)/\Delta t \qquad (3)$$

so long as the phytoplankton suspension is not being diluted by phytoplankton-free media over the period, Δt. Eq. 3 implies that temporal changes in r can be visualized by plotting phytoplankton biomass on a logarithmic scale against time. In Fig. 2A, the C_{phyt} record is plotted on a logarithmic scale for bin NA-5 (red box in Fig. 1A). From this plot, it is immediately apparent that C_{phyt} begins to increase in the middle of winter, not in the spring. (Vertical dashed lines in Fig. 2A indicate 1 January.) Moreover, the rate of increase (i.e., the slope of $\log(C_{phyt})$ vs. time) is highly constrained throughout the winter-through-spring period in most cases (Fig. 2A).

In Fig. 2B–F, mean seasonal cycles in C_{phyt} (black symbols) for bins NA-2, NA-5, NA-8, NA-11, and NA-12 are compared to coincident changes in MLD (solid black line; note that these five bins correspond to the heavy black box in Fig. 1A). These five plots illustrate latitudinal similarities and differences in mean annual phytoplankton cycles. In each case, C_{phyt} is already increasing when MLDs are at their maximum. Similar results are found for all 12 bins for both C_{phyt} and Chl_{sat} (Appendix: Fig. A2). Indeed, in 104 out of the total 108 annual cycles available for the 12 bins, the onset of net positive growth in C_{phyt} is found to coincide with the cessation of mixed layer deepening. In no case is positive net growth delayed until significant shoaling of the mixed layer occurs. Furthermore, alternative sources of MLD estimates all yield consistent relationships between C_{phyt} and MLD (gray symbols and standard error bars in Fig. 2B–F; see figure legend for details).

The satellite record clearly indicates that North Atlantic bloom initiation is not a springtime event, but rather occurs in midwinter, at the latest. This finding strongly refutes the Critical Depth Hypothesis, but raises the new question: "Why does cessation of mixed layer deepening initiate a net increase in phytoplankton
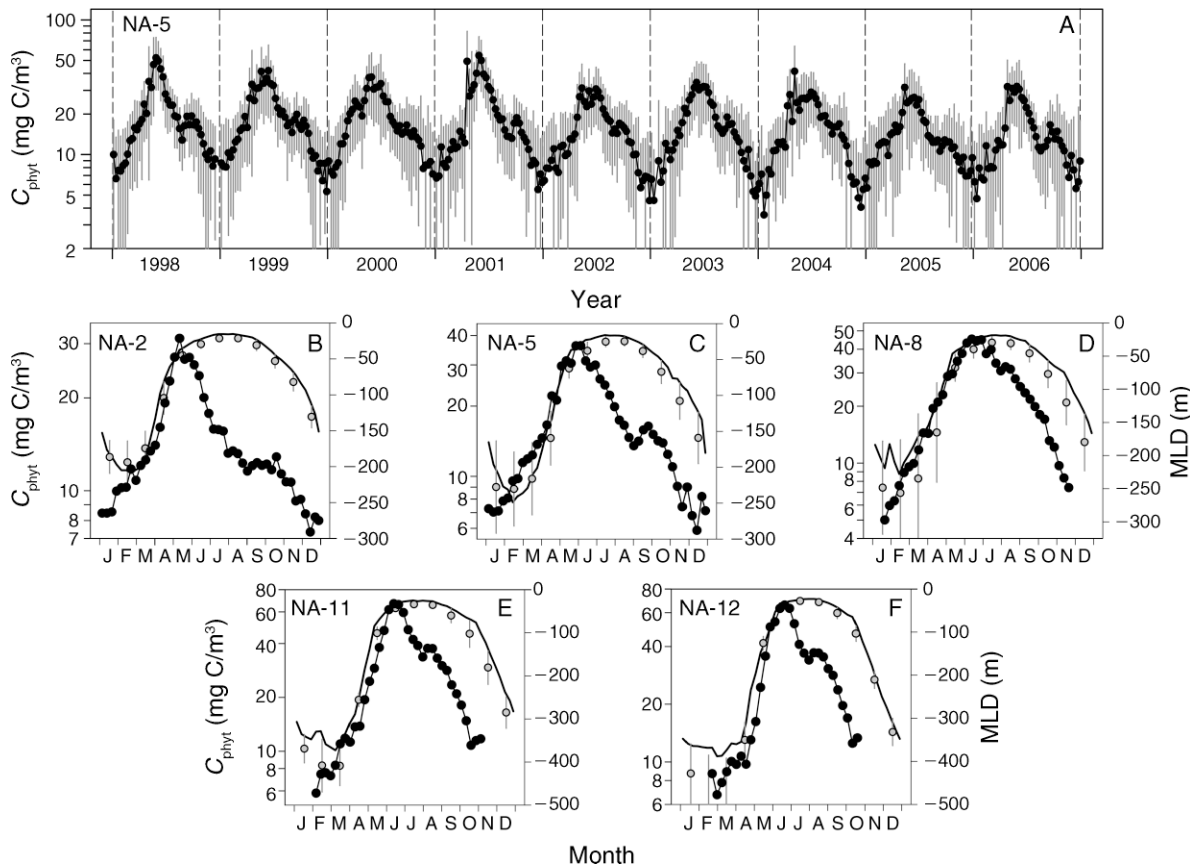
FIG. 2. (A) Nine-year record of phytoplankton biomass (C_{phyt}) at eight-day resolution for bin NA-5 plotted with a log-transformed y-axis (same data as in Fig. 1B, C). Gray bars indicate within-bin standard deviations. Vertical dashed lines indicate 1 January of each year. (B–F) Mean annual cycles in C_{phyt} at eight-day resolution (black symbols, log-transformed left axis) and mixed layer depth (MLD) from the Fleet Numerical Meteorology and Oceanography Center (FNMOC) and the Simple Ocean Data Assimilation (SODA) models (black line, right axis). Gray symbols (right axis) represent mean mixed layer depth for three models, showing close agreement in timing of mixed layer deepening and shoaling despite differences in magnitude of midwinter mixing depth (gray bars indicate standard deviation between models). The three MLD estimates are from the FNMOC/SODA model (as in Fig. 1), the Miami Isopycnic Coordinate Ocean Model (MICOM; Bleck et al. 1992), and a higher resolution (20–40 km) version of the MICOM (Hátún et al. 2005; see Milutinović et al [2009] for additional details). Annual cycles begin in January and end in December (x-axes).

concentration?" To answer to this question, it is important to recognize (as alluded to previously) that net phytoplankton specific growth rates are not accurately reflected by changes in carbon concentration when a population is being diluted. A quintessential example of this issue is a chemostat culture, where growth rate is equivalent to dilution rate and independent of biomass (which is held constant). As explained by Evans and Parslow (1985), dilution effects must be considered in the North Atlantic when mixed layer deepening entrains phytoplankton-free water from below. If this dilution effect is sufficiently large, it is possible for phytoplankton concentration to decrease (e.g., in late autumn and early winter) despite net in situ population growth. To achieve a more complete understanding of North Atlantic seasonal phytoplankton cycles, it is therefore necessary to first account for dilution effects and then evaluate variability in r directly

(as opposed to simply viewing log-transformed plots of C_{phyt}). To conduct such an analysis using satellite data, Eq. 3 can be used to estimate r from changes in C_{phyt} during periods of mixed layer shoaling and when mixed layer deepening entrains significant phytoplankton biomass from below. During periods when mixing entrains relatively phytoplankton-free water, r must instead be estimated from changes in mixed layer integrated phytoplankton biomass ($\Sigma C_{phyt} = C_{phyt} \times$ MLD; expressed as mg C/m^2), which accounts for dilution of the population over a larger volume.

For the current study, r was estimated from ΣC_{phyt} whenever MLD exceeded the euphotic depth (Z_{eu} = depth to which 1% of surface irradiance penetrates). This criterion was chosen because global field data sets (e.g., Behrenfeld and Falkowski 1997) show phytoplankton biomass throughout the euphotic zone when MLD < Z_{eu}, while chlorophyll profiles in the North
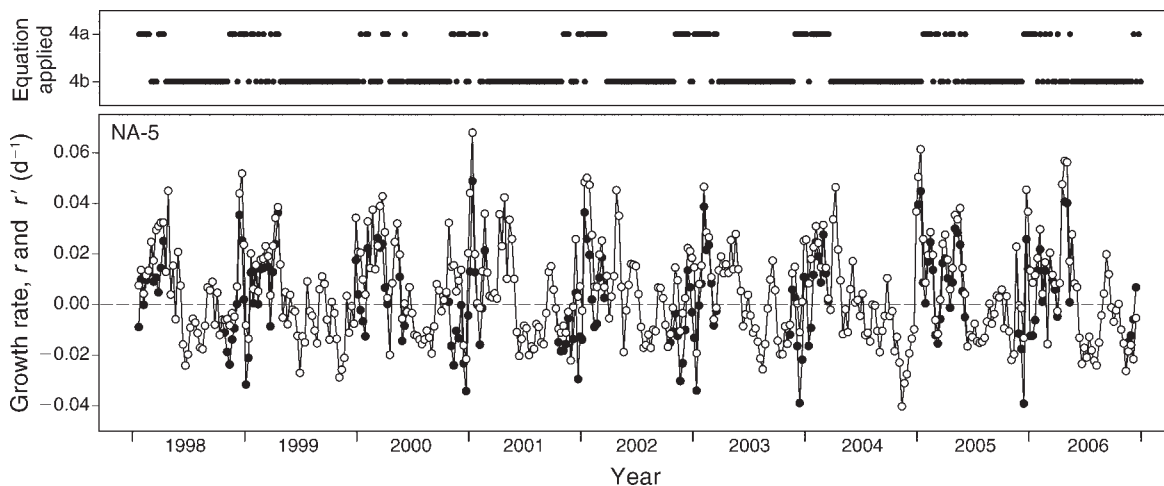
FIG. 3. Nine-year record of phytoplankton net specific growth rate (r; open symbols) for bin NA-5. Also shown are net growth rates that would result if dilution effects of mixed layer deepening were not accounted for (r', solid symbols). This r' is equivalent to applying Eq. 4b to all the data in Fig. 2A. A three-bin running boxcar averaging has been applied to dampen high frequency variability. Upper panel: dots indicate where Eqs. 4a and 4b were applied for calculating r for each eight-day period.

Atlantic indicate sharp decreases below the mixed layer during periods of deep mixing when MLD $> Z_{eu}$ (Ward and Waniek 2007). Thus, r was calculated from eight-day resolution satellite data for each North Atlantic bin following

$$r = \ln\left(\sum C_{phyt-1}\Big/\sum C_{phyt-0}\right)\Big/\Delta t;$$

$$\text{if MLD is deepening and} > Z_{eu} \quad (4a)$$

$$r = \ln(C_{phyt-1}/C_{phyt-0})/\Delta t;$$

$$\text{if MLD is shoaling or} < Z_{eu} \quad (4b)$$

where C_{phyt-0} and $\Sigma\, C_{phyt-0}$ are initial biomass levels and C_{phyt-1} and $\Sigma\, C_{phyt-1}$ are biomass levels after the time interval, $\Delta t =$ eight days. As a noteworthy aside, Eq. 4a provides an accurate assessment of r if mixed layer deepening entrains phytoplankton-free water from depth and dilution is complete (which seems a reasonable assumption given mixed layer transit times of a few days or less; Backhaus et al. 2003, D'Asaro 2008). Eq. 4b, on the other hand, would provide an accurate estimate of r if the deep water entrained by mixing had a phytoplankton concentration equivalent to the initial surface population. Thus, the true value of r is bounded by Eqs. 4a and 4b if entrained deep water is not entirely devoid of phytoplankton. This uncertainty influences the confidence that can be assigned to retrieved values of r for any given eight-day period, but has little impact on the overall pattern in r across the mixed layer deepening period where MLDs increase by hundreds of meters and the clear water assumption for deep water is a reasonable approximation (Ward and Waniek 2007).

In Fig. 3, the nine-year record of r based on Eqs. 4a and 4b is shown for bin NA-5 (open symbols). Fig. 3

also shows net specific rates of change in biomass based on C_{phyt} alone ($r' =$ black symbols). In other words, r' represents the net specific growth rates that would result if dilution effects of mixed layer deepening were ignored and Eq. 4b was applied to all the data in Fig. 2A. This comparison illustrates a few important points. First, seasonal cycles and variability in r and r' are highly correlated ($r = 0.90$), indicating that overall patterns and variability across the nine-year record are robust to the approach for calculating r. Second, the dilution correction (Eq. 4a) is generally modest and only impacts r during a short period of late autumn and early winter (upper panel of Fig. 3), implying that the uncertainties in deep water phytoplankton concentrations described above do not compromise basic findings described herein. Finally, the primary influence of the dilution correction is that it advances the period of positive net population growth to slightly earlier in the year, but initiation of this positive growth phase is found in midwinter whether based on r or r'. Again, this conclusion is illustrated in Fig. 2 by the increases in C_{phyt} observed from January onward.

In Fig. 4A, the nine-year record of r for bin NA-5 (same data as in Fig. 3, open symbols) is plotted along with coincident changes in PAR (gray line, lower right axis) and MLD (black line, upper right axis; note that values increase upward). Here we see that during each seasonal cycle r is negative over most of the summer and early autumn, then increases in parallel with increasing MLD and decreasing PAR to become positive by late autumn (horizontal dashed line indicates $r = 0$), and thereafter remains positive until early summer (Fig. 4A). For all eight complete seasonal cycles at NA-5, this positive growth phase begins while PAR is decreasing and, on average, precedes the post-solstice increase in PAR by 45 days (range 16–80 days). Clearly, the
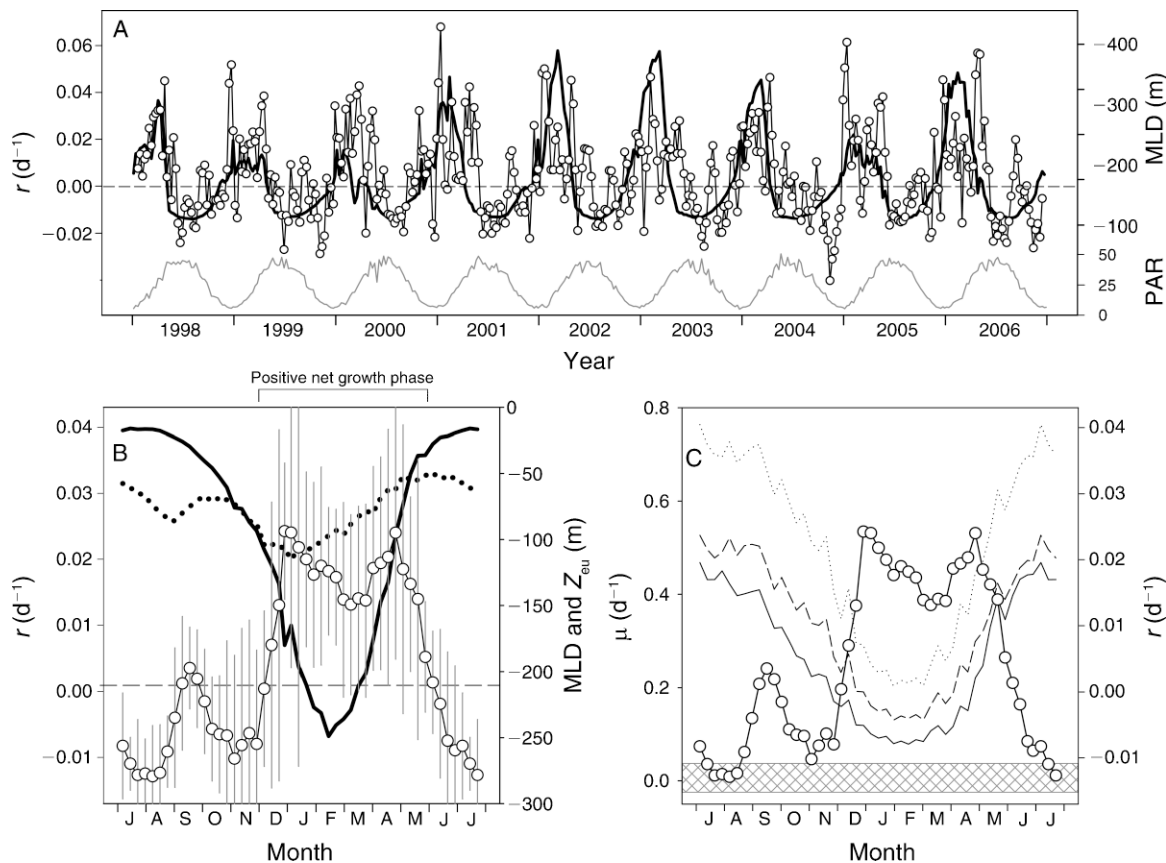
Fig. 4. (A) Nine-year record of phytoplankton net specific growth rate (r; open symbols, left axis = same data as open symbols in Fig. 3), mixed layer depth (MLD; heavy black line, upper right axis), and photosynthetically active radiation (PAR: light gray line, lower right axis). Note that MLD increases upward in this figure to illustrate correlation with r. All data are at eight-day resolution. A three-bin running boxcar averaging has been applied to r to dampen high frequency variability. (B) Annual mean cycles from July to following July of r (open symbols, left axis), MLD (heavy black line, right axis), and euphotic depth (Z_{eu}: heavy dotted line, right axis) for bin NA-5. Note that in this figure MLD increases downward. Gray bars indicate standard deviation in r for each eight-day period over the nine-year satellite record (panel A). "Positive net growth phase" is indicated at top. Horizontal dashed line indicates $r = 0$. (C) Annual mean cycles in phytoplankton specific growth rate (μ) for NA-5 (left axis) based on net primary production (NPP) estimates from (solid line) the standard Vertically Generalized Production Model (VGPM); (dashed line) the VGPM with an exponential description of chlorophyll-specific light-saturated photosynthesis (P_{opt}^{b}); and (dotted line) the VGPM with a regionally tuned description of P_{opt}^{b} (see the *Abandoning Sverdrup* section for details). Note again that the x-axis begins in July and ends in July a year later. Also shown is the mean annual cycle in r from panel B (open symbols, right axis, with same scale as in panel B). Gray hatched box shows where the entire annual range in r is found when plotted on the same left axis as μ, emphasizing how small r is relative to μ throughout the year.

positive net growth phase is not initiated by increasing PAR or mixed layer shoaling. The NA-5 record also illustrates the high temporal variability in r and shows that the peak in r is not consistently found in spring. For example, a spring peak in r is found during 2005–2006, but the peak during 2000–2001 and 2002–2003 occurs during midwinter and prior to the MLD shoaling (Fig. 4A). During some years, there is no clear peak in r throughout the positive growth phase (e.g., 1999–2000), while in other years similar magnitude peaks in r are found in midwinter and spring (e.g., 1998–1999 and 2001–2002; Fig. 4A). Similar variability is found for the other North Atlantic bins, but the overall pattern that emerges is consistent: the spring maximum in phytoplankton concentration represents the culmination of a

positive population growth phase that begins during late autumn/winter. This positive growth phase is initiated during mixed layer deepening and is first expressed as an increase in C_{phyt} (and Chl_{sat}) when deep-water entrainment into the mixed layer stops (i.e., dilution; Fig. 2; Appendix: Fig. A2).

In Fig. 4B, the mean annual cycle for r at NA-5 is shown (open symbols), along with mean values for MLD and Z_{eu} (note that in this figure the x-axis begins with July and MLD increases downward on the right axis). Here we see that the positive growth phase (December to June) begins roughly when the mixed layer penetrates below the euphotic layer (i.e., MLD > Z_{eu}; Fig. 3B). This correspondence is also found in the other bins with complete satellite coverage over the

annual cycle and does not simply reflect the criteria described above for estimating r, as it is also found if r is estimated from ΣC_{phyt} whenever MLD is increasing (i.e., if the MLD $> Z_{eu}$ criteria is dropped in Eq. 4a). Another characteristic of the mean annual cycles in r is a slight midwinter depression (e.g., January through March in Fig. 4B), which becomes more prominent at higher latitudes and gives the positive growth phase a "dual peaked" appearance (Fig. 4B). The mean annual cycle also shows the small and brief positive growth period associated with the September–October "fall bloom" (Fig. 4B).

With the satellite record of net population growth rates in the North Atlantic (Fig. 4A, B), we can now dismiss the Critical Depth Hypothesis as a valid explanation for bloom initiation. To better understand how a positive growth phase can persist during winter when PAR is low and MLDs are maximal, it is instructive to compare absolute values of r with coincident variations in phytoplankton specific growth rates (μ). To estimate μ, net primary production (NPP) was calculated from satellite Chl_{sat} data using three approaches: (1) the standard parameterization of the Vertically Generalized Production Model (VGPM; Behrenfeld and Falkowski 1997), (2) the VGPM with an exponential function describing chlorophyll-specific light-saturated photosynthesis (P^b_{opt}) following Morel (1991), and (3) the VGPM with a regionally tuned estimate of P^b_{opt}. The first two of these approaches are described in Campbell et al. (2002) and were found in the round-robin algorithm testing study of Carr et al. (2006) to be representative of the two major categories of satellite NPP estimates. In the third approach, phytoplankton Chl:C ratios were described as a function of mixed layer light level following Behrenfeld et al. (2005) and P^b_{opt} described as an inverse function of Chl:C ratio and tuned to give values consistent with measured P^b_{opt} during the North Atlantic Bloom Experiment (*available online*).[3] All three models give NPP estimates per square meter, which were then divided by active phytoplankton biomass (i.e., integrated carbon from the surface to the greater of Z_{eu} and MLD) to estimate μ.

In Fig. 4C, seasonal cycles in μ are shown for NA-5. Despite differing magnitudes, all three models give similar seasonal cycles because changes in NPP (thus μ) are dominated by changes in Chl_{sat} and PAR. Also shown in Fig. 4C and plotted on the right hand axis is the seasonal cycle in r from Fig. 4B (open symbols). This comparison illustrates the general inverse relationship between μ and r and strongly implies that the positive growth phase leading to the spring peak in phytoplankton biomass is less a consequence of springtime increases in μ as it is a reflection of seasonal changes in loss rates (l). In other words, the only way for r to increase while μ is decreasing is for the fraction of μ escaping losses to

increases as μ decreases. To clearly understand this finding, it is important to recognize in Fig. 4C the very different scales for μ (left axis) and r (right axis). If instead both properties were plotted on the left axis, the full seasonal cycle in r would fall within the hatched box at the bottom of the figure. This comparison illustrates why the positive growth phase can persist throughout the winter: r is so small that it requires very little NPP to support it (Fig. 4C). Indeed, the mean value of r from mid-December to mid-April at NA-5 is only 0.018/d, corresponding to a population doubling time of more than a month. Again, the essential requirement to achieve comparable values of r from winter through spring (Fig. 4B) is that phytoplankton loss rates (l) must covary closely with μ, and herein lies the crucial flaw in the Critical Depth Hypothesis: Sverdrup assumed l to be constant over time.

THE DILUTION–RECOUPLING HYPOTHESIS

The annual North Atlantic phytoplankton bloom is the consequence of a decoupling between phytoplankton growth and losses (Eqs. 1, 2) and it terminates with either the exhaustion of surface nutrients or overgrazing by heterotrophs (Banse 1992, 2002). The key question is whether this decoupling is due to increased phytoplankton growth rates or decreased losses (Eq. 1). As described above, the positive net growth phase of the annual cycle leading to the late spring climax in biomass starts in late winter (Fig. 4), which dismisses the Critical Depth Hypothesis as a valid explanation for bloom initiation. Onset of the positive phase also coincides with decreasing incident irradiance and, in general, r is found to be inversely related to PAR, NPP, and μ. These observations deemphasize the importance of the spring stimulation in phytoplankton photosynthesis and growth, and emphasize the importance of seasonal perturbations in the loss terms for phytoplankton biomass (Banse 1992). In this section, I propose a Dilution–Recoupling Hypothesis for the North Atlantic bloom that focuses on physical processes impacting phytoplankton growth–loss relationships, incorporates seasonal changes in μ, and builds upon the earlier work of Evans and Parslow (1985), Banse (1992, 2002), and Marra and Barber (2005). While the hypothesis provides a framework for understanding the North Atlantic seasonal phytoplankton cycle and is consistent with the satellite observations (Figs. 2–4), it is only a hypothesis and other interpretations and complexities should be considered in the future. It is also important to recognize that satellite data provide limited information for distinguishing different loss terms for phytoplankton biomass. Thus, in the words of Sverdrup, "It is not advisable to place too great emphasis on the agreement between theory and observation."

Eq. 2 captures the primary loss terms influencing r. Of these, the "flushing" term (f) can be dismissed as a significant factor influencing retrieved values of r because the large bin sizes used in the current analysis

[3] ⟨http://usjgofs.whoi.edu/jg/dir/jgofs/⟩

minimize the horizontal advection effects between any two eight-day sampling periods and the impact of dilution from mixed layer deepening has been accounted for in calculations of r. Seasonal changes in sinking losses (s), on the other hand, can contribute to the annual phytoplankton cycle. During mixed layer deepening, vertically exported phytoplankton can be entrained back into the surface layer (Ward and Waniek 2007). Seasonal changes in taxonomy also occur, with smaller, slow sinking (often flagellated) species dominating during winter and more rapidly sinking diatoms becoming prevalent later in the bloom (Halldal 1953, Paasche 1960, Ramsfjell 1960, Paasche and Rom 1962, Parsons and Lalli 1988, Dale et al. 1999, Backhaus et al. 2003, Ward and Waniek 2007). Aggregate formation can also significantly increase s during later stages of the bloom, as coagulation increases as a squared function of particle concentration, and may even set a limit to maximum achievable bloom concentrations (Jackson 2005). Much less is known about seasonal changes in viral infection and parasitism in the North Atlantic. However, while many factors clearly contribute to phytoplankton losses, grazing (g) is by far the dominant term at most times (e.g., Steemann Nielsen 1957, Banse 1992, Banse and English 1994) and, importantly, g can respond rapidly to changes in phytoplankton biomass and μ. Accordingly, the Dilution–Recoupling Hypothesis focuses on phytoplankton–grazer interactions and physical processes perturbing the balance between μ and g. To begin, a brief digression is helpful regarding effects of dilution.

In planktonic ecosystems, the impact of dilution on predator–prey interactions is commonly exploited for assessing phytoplankton specific growth rates (μ). The technique is referred to as a "dilution experiment" (Landry and Hassett 1982, Landry 1993, Landry et al. 1995). A dilution experiment is conducted by dispensing different ratios of whole and filtered seawater into vessels of equal size, measuring initial concentrations of chlorophyll, incubating the samples for some time period, and then assessing final chlorophyll concentrations at the end of the incubation (Landry and Hassett 1982, Landry et al. 1995). Phytoplankton net specific growth rates (r) are then calculated (Eq. 3) for each treatment and plotted against dilution ratio. The resultant relationship typically shows r increasing linearly with dilution (e.g., Landry et al. 1995), although other nonlinear relationships are possible (Evans and Paranjape 1992). Extrapolation of this relationship to the intercept provides the estimate of μ. The dilution experiment works because addition of filtered seawater to whole seawater decreases l by diluting predators and prey (i.e., changes predator–prey encounter rates), but ideally does not alter μ (Landry and Hassett 1982). Importantly, relatively short incubations (~1 day) are employed to prevent predator and prey population growth from negating the impact of the dilution procedure. In other words, the dilution effect is transient. To sustain this effect over a much longer period, new filtered seawater would need to be added at a rate comparable to population growth rates (thus maintaining constant predator–prey interactions). The relevance of this small volume experimental technique to plankton dynamics of the subarctic North Atlantic basin is that it provides a tangible example of a simple process altering the balance between μ and l that occurs naturally over vast areas during mixed layer deepening.

The underlying concept of the Dilution–Recoupling Hypothesis is that the complex heterotrophic food web of planktonic ecosystems allows a constant tight coupling (rapid response time) between phytoplankton growth and losses, but seasonal mixed layer deepening has the potential to slightly decouple μ and g by impacting predator–prey interactions through dilution of both phytoplankton and grazers (as in a dilution experiment). A strong tendency for g to balance μ implies that this decoupling effect will only be maintained through continued dilution. Thus, cessation of mixed layer deepening should advocate a strengthening in predator–prey coupling. As described in the modeling study of Evans and Parslow (1985), this recoupling can be further enhanced by mixed layer shoaling, which both severs nonmobile phytoplankton at depth from the photic zone (Backhaus et al. 2003) and concentrates the mobile grazing community into a shrinking "photosynthetically active" volume (i.e., the surface mixed layer or euphotic zone). The following paragraph applies these basic concepts to narrate one potential interpretation of the repeated seasonal cycles in r resolved from the SeaWiFS data and illustrated in Fig. 4.

Starting in late spring, surface nutrient depletion or overgrazing terminates the annual North Atlantic bloom (Banse 1992, 2002). From this point through the remaining stratified summer months, losses (grazing, sinking, others) exceed μ, with biomass decreasing roughly exponentially (Fig. 2) at a specific rate between $r = 0$ and $r = -0.01$ per day (Fig. 4). In late summer and early autumn, the mixed layer begins to penetrate deeper reaches of the euphotic zone, entraining nutrients as well as phytoplankton and grazers from below. During this period, the "dilution effect" is minimal (i.e., predator–prey encounter rates are not strongly altered) and only minor changes in r are observed (Fig. 4B, September–October) that largely reflect nutrient-driven changes in μ. Eventually, however, mixed layer deepening begins to entrain relatively plankton-free water from below. This event roughly coincides with MLD > Z_{eu} (Fig. 4B, November–December) and, according to the scenario described above, perturbs the balance between μ and g (as in a dilution experiment) and initiates the positive net growth phase and the annual North Atlantic bloom (Fig. 4B). The start of this positive r phase corresponds to an increase in areal biomass (ΣC_{phyt}) but not necessarily phytoplankton concentration (C_{phyt}; m^{-3}) because gains in biomass are being distributed over a growing volume of water (i.e., MLD is still increasing).

Once the mixed layer stops deepening, though, the positive population growth rate becomes apparent in C_{phyt}, resulting in the observed coincidence between initial increases in C_{phyt} and cessation of mixed layer deepening (Fig. 2). From this point forward to the end of bloom, grazing pressure increases (because decoupling by dilution has ended) but is countered by light-driven increases in μ, allowing r to remain high (even increase) well into the spring (Fig. 4). Importantly, this scenario does not require stratification for a bloom to occur (Evans and Parslow 1985), only cessation of mixed layer deepening, making this new view compatible with observations of bloom development in the absence of shoaling (Heimdal 1974, Schei 1974, Townsend et al. 1992, Eilertsen 1993, Backhaus et al. 1999, Dale et al. 1999). Nevertheless, stratification does have two significant impacts on the North Atlantic bloom under the Dilution–Recoupling Hypothesis: it accelerates the spring increase in grazing pressure within the mixed layer by concentrating mobile heterotrophs (Evans and Parslow 1985), while simultaneously increasing μ through improvements in median mixed layer light levels (Reynolds 2006). Thus, springtime increases in μ retain an important role by prolonging the positive growth phase despite stratification-driven increases in g, as well as biomass-driven increases in s (Jackson 2005).

The Dilution–Recoupling Hypothesis narrated above largely focuses on only two terms in Eq. 2: μ and g. Despite this shortcoming, it does appear to account for fundamental features in the seasonal cycle in r and it also provides a useful context for interpreting additional features of the satellite data. For example, as an extension of field dilution experiments, the Dilution–Recoupling Hypothesis assumes that predator–prey decoupling from mixed layer deepening results from changes in predator and prey concentrations, not from changes in μ. Accordingly, when r is expressed as a fraction of μ using data in Fig. 4C (i.e., r/μ), this fraction is found to increase and decrease in parallel with MLD deepening and shoaling ($r = 0.91$, data not shown), without the midwinter depression observed in r (Fig. 4B, C). The same result is found for all 12 bins (mean $r = 0.87$). Thus the typical "dual peaked" appearance in mean seasonal cycles of r (Fig. 4B, C) can be interpreted as reflecting changes in the balance between mixed layer effects on l and light-driven effects on μ. Similarly, latitudinal changes in this balance resulting from different seasonal cycles in MLD and incident light can be related to the more pronounced midwinter depressions in r noted earlier for higher latitude bins. Finally, comparison of satellite-derived r and μ for the 12 bins consistently indicates that the decoupling of μ and l from mixed layer deepening is roughly twice as large as the recoupling effect from an equivalent shoaling of the mixed layer. This finding is consistent with the "asymmetric effect" envisioned by Evans and Parslow (1985) to result from mixed layer deepening

diluting both predators and prey, while mixed layer shoaling primarily concentrates predators alone.

CONCLUSION

The North Atlantic phytoplankton bloom is among the most conspicuous features in the global satellite record and has been a topic of ecological interest for over a century (see Banse 1992). The appearance of elevated phytoplankton concentrations coinciding with springtime improvements in upper ocean growth conditions (light, temperature, stratification) led early on to the assumption that the vernal bloom was a consequence of increased phytoplankton growth rates. Sverdrup's Critical Depth Hypothesis subsequently provided a framework for understanding the environmental conditions necessary to initiate a bloom, and this hypothesis has served the ecological science community for over half a century. Today, satellite observations provide coverage of the North Atlantic bloom in a manner unimaginable in Sverdrup's time and, with these data, basic assumptions of the Critical Depth Hypothesis are found wanting. Results presented here demonstrate that bloom initiation occurs in the winter when mixed layer depths are maximum (Figs. 2, 4), that the coupling between phytoplankton growth and losses increases rather than decreases during spring stratification (Fig. 4C), that annual maxima in net population growth rates are as likely to occur in midwinter as in spring (Fig. 4A), and that phytoplankton loss rates are not constant (as assumed by Sverdrup), but proportional to, and perpetually coupled tightly with, phytoplankton growth rates. The current analysis also shows that the positive net growth phase in the North Atlantic begins prior to an increase in light and generally occurs while mixing depths are still increasing. With these findings it is necessary to abandon the notion that the bloom simply reflects an increase in phytoplankton division rate. Indeed, the satellite record indicates an overall inverse relationship between r and μ (Fig. 4C). That net growth rate can exhibit the opposite sign of cell division rate was earlier acknowledged, for example, by Riley (1946), Margalef et al. (1957), and Banse (2002).

As a replacement for the Critical Depth Hypothesis, a Dilution–Recoupling Hypothesis is outlined here that focuses on the balance between phytoplankton growth and grazing, and seasonally varying physical processes influencing this balance. The central role of grazing on phytoplankton population dynamics has been recognized (yet often overlooked) since the mid-20th century (see discussion in Banse 1992:428–430), but a complete understanding of the annual cycle in phytoplankton–grazer interactions has been hindered by infrequent sampling and a bias in field campaigns toward late stages of the bloom. Fortunately, satellite observations already provide the necessary measurement frequency to begin resolving temporal aspects of plankton dynamics in the seasonal seas. The Dilution–Recoupling Hypothesis described here adopts concepts from Evans and

Parslow (1985) and distinguishes two primary impacts of MLD changes on the balance between μ and l. In the "dilution phase," mixed layer deepening lowers predator and prey concentrations and thus weakens the link between μ and g by reducing encounter rates. In the "recoupling phase," the tendency of planktonic ecosystems to balance μ and l is favored. During this phase, g increases relative to μ because the decoupling period of mixed layer deepening has ended. Importantly, mixed layer shoaling is not requisite for the bloom, but instead intensifies g by concentrating mobile predators into a shrinking volume, which is offset by concurrent increases in μ (Reynolds 2006). With or without stratification, springtime increases in PAR are critical to maintain μ above a growing grazing pressure. At very high latitudes, spring increases in PAR are particularly important because they also mark the end of polar night and thus permit growth.

The broader applicability of the Dilution–Recoupling Hypothesis to other environments remains to be tested. However, the impact of mixed layer deepening on r through dilution of phytoplankton and grazers as described by Evans and Parslow (1985) was recently applied to studies on monsoon-driven blooms in the Arabian Sea by Marra and Barber (2005). In this case, the authors adopt the Critical Depth Hypothesis, but argue that seasonal mixing is inadequate for light limitation of phytoplankton growth (Barber et al. 2001, Marra and Barber 2005). Nitrogen is likewise dismissed as a limiting factor for μ in the Arabian Sea. The appearance of elevated biomass following monsoon-driven erosion of the mixed layer was therefore proposed to result from dilution effects on grazing (Marra and Barber 2005), as per Evans and Parslow (1985). J. Marra and T. S. Moore, II, *unpublished manuscript*, have since insightfully stated that "monsoon-induced vertical mixing is more a factor in resource limitation for the micrograzers than the phytoplankton," but they also make a distinction that "In the Arabian Sea, unlike the North Atlantic, . . . mixing never exceeds the critical depth." While this later statement is clearly challenged herein, the modeling work of Evans and Parslow (1985), the Arabian Sea study of Marra and Barber (2005), and the North Atlantic analysis of the current study are all converging, at a fundamental level, toward a consistent view of seasonal plankton dynamics dominated by physical disruption and ecological recoupling of phytoplankton–grazer interactions.

The primary motivation for this effort has been to invigorate discussion on seasonal phytoplankton blooms and, at the very least, give the reader some pause to accepting traditional interpretations. The Dilution–Recoupling Hypothesis, at best, provides a basic framework regarding first-order properties of the North Atlantic bloom. Clearly, the current treatment fails to address many of the ecological complexities regarding North Atlantic plankton, including species successions, short-term variability in r (Fig. 4A), and the basis for

temporal stability in r from winter through spring (Fig. 2). As work continues along these lines, a shift in focus is strongly recommended that emphasizes variability in r and seasonal changes in r as a fraction of μ, rather than simply focusing on standing stock. This recommendation is intended to assist in understanding seasonal plankton dynamics, not to discount the significance of biomass accumulation. Indeed, higher trophic-level fertility of the North Atlantic is linked to the vernal period of the bloom, as is seasonal pCO_2 draw down associated with organic carbon export. Nevertheless, population changes preceding the vernal climax and imprinted in the record of r play a crucial role in setting the stage for the event. Resolving these processes will require a break from traditional late-bloom field studies, development of a balanced research program covering the full annual cycle, and the employment of new high-temporal-resolution technologies capable of prolonged deployment (e.g., Boss et al. 2008). The significance of this revised philosophy was elegantly stated by Evans and Parslow (1985): "Observations that phytoplankton [are] abundant for a short period almost every spring . . . implies that the ecosystem not only produces a bloom in the spring but also recreates, over the fall and winter, the conditions necessary for a bloom. A spring bloom is not an isolated event, but one feature of a roughly repeating annual cycle."

A correct understanding of plankton dynamics throughout the annual cycle and the mechanisms underlying this succession of events is particularly essential today for interpreting current observed trends and forecasting future change. For example, if one adopts the notion that a vernal bloom emerges from elevated phytoplankton growth rates (μ) resulting from mixed layer shoaling above a critical depth, then increased stratification from climate warming may be anticipated to enhance North Atlantic blooms (or at least advance their timing to earlier spring). In contrast, the Dilution–Recoupling Hypothesis described here emphasizes the crucial role of mixing on the seasonal decoupling of μ and g. According to this view, deep mixing is essential for bloom formation, with deeper mixing causing greater perturbations to predator–prey interactions than shallower mixing. Consistent with this notion, higher latitudes of the North Atlantic are found to have deeper winter mixing (Fig. 2), a greater winter decoupling of μ and l, higher winter-to-spring values of r (Appendix: Fig. A3, panel A), and higher peak chlorophyll concentrations (Appendix: Fig. A3, panel B). Extending this Dilution–Recoupling Hypothesis to climate warming suggests that suppression of winter mixing may lead to reduced net phytoplankton growth rates and vernal biomass (i.e., an opposite conclusion from one based on the Critical Depth Hypothesis). Interestingly, the satellite record to date shows an inverse relationship between sea surface temperature changes and Chl$_{sat}$ at high latitudes (Behrenfeld et al. 2008, 2009).

Literature Cited

Backhaus, J. O., E. Hegseth, H. Wehde, X. Irigoien, K. Hatten, and K. Logemann. 2003. Convection and primary production in winter. Marine Ecology Progress Series 215:1–14.

Backhaus, J., H. Wehde, E. N. Hegseth, and J. Kämpf. 1999. "Phytoconvection"—on the role of oceanic convection in primary production. Marine Ecology Progress Series 189: 77–92.

Banse, K. 1992. Grazing, temporal changes of phytoplankton concentrations, and the microbial loop in the open sea. Pages 409–440 in P. G. Falkowski and A. D. Woodhead, editors. Primary productivity and biogeochemical cycles in the sea. Plenum Press, New York, New York, USA.

Banse, K. 1994. Grazing and zooplankton production as key controls of phytoplankton production in the open ocean. Oceanography 7:13–20.

Banse, K. 2002. Steeman Nielsen and the zooplankton. Hydrobiology 480:15–28.

Banse, K., and D. C. English. 1994. Seasonality of coastal zone color scanner phytoplankton pigment in the offshore oceans. Journal of Geophysical Research 99:7323–7345.

Barber, R. T., J. Marra, R. R. Bidigare, L. A. Codispoti, D. Halpern, Z. Johnson, M. Latasa, R. Goericke, and S. L. Smith. 2001. Primary productivity and its regulation in the Arabian Sea during 1995. Deep-Sea Research II 48:1127–1172.

Behrenfeld, M. J., and E. Boss. 2003. The beam attenuation to chlorophyll ratio: an optical index of phytoplankton photoacclimation in the surface ocean? Deep Sea Research 50: 1537–1549.

Behrenfeld, M. J., and E. Boss. 2006. Beam attenuation and chlorophyll concentration as alternative optical indices of phytoplankton biomass. Journal of Marine Research 64: 431–451.

Behrenfeld, M. J., E. Boss, D. A. Siegel, and D. M. Shea. 2005. Carbon-based ocean productivity and phytoplankton physiology from space. Global Biogeochemical Cycles 19: GB1006.

Behrenfeld, M. J., and P. G. Falkowski. 1997. Photosynthetic rates derived from satellite-based chlorophyll concentration. Limnology and Oceanography 42:1–20.

Behrenfeld, M. J., D. A. Siegel, and R. T. O'Malley. 2008. Global ocean phytoplankton and productivity. Pages S56–S61 in J. M. Levy, editor. State of the climate in 2007. Bulletin of the American Meteorlogical Society, July 2008.

Behrenfeld, M. J., D. A. Siegel, R. T. O'Malley, and S. Maritorena. 2009. Global ocean phytoplankton. Pages 568–573 in T. C. Peterson and M. O. Baringer, editors. State of the climate in 2008. Bulletin of the American Meteorlogical Society, August 2009.

Bleck, R., C. Rooth, D. Hu, and L. T. Smith. 1992. Salinity-driven thermocline transients in a wind- and thermohaline-forced isopycnic coordinate model of the North Atlantic. Journal of Physiological Oceanography 22:1486–1505.

Boss, E., D. Swift, L. Taylor, P. Brickley, R. Zaneveld, S. Riser, M. J. Perry, and P. G. Strutton. 2008. Observations of pigment and particle distributions in the Western North Atlantic from an autonomous float and ocean color satellite. Limnology and Oceanography 53:2112–2122.

Campbell, J., et al. 2002. Comparison of algorithms for estimating primary productivity from surface chlorophyll, temperature and irradiance. Global Biogeochemical Cycles 16(3):10.1029.

Carr, M.-E., et al. 2006. A comparison of global estimates of marine primary production from ocean color. Deep Sea Research 53:741–770.

Clancy, R. M., and W. D. Sadler. 1992. The fleet numerical oceanography center suite of oceanographic models and products. Weather and Forecasting 7:307–327.

Crumpton, W. G., and R. G. Wetzel. 1982. Effects of differential growth and mortality in the seasonal succession of phytoplankton populations in Lawrence Lake, Michigan. Ecology 63:1729–1739.

Dale, T., F. Rey, and B. R. Heimdal. 1999. Seasonal development of phytoplankton at a high latitude ocean site. Sarsia 84:1–17.

Dall'Olmo, G., T. K. Westberry, M. J. Behrenfeld, E. Boss, and W. Slade. 2009. Significant contribution of large particles to optical backscattering in the open ocean. Biogeosciences 6: 947–967.

D'Asaro, E. A. 2008. Convection and the seeding of the North Atlantic bloom. Journal of Marine Systematics 69:233–237.

Ellertsen, H. C. 1993. Spring blooms and stratification. Nature 363:24.

Evans, G. T., and M. A. Paranjape. 1992. Precision of estimates of phytoplankton growth and microzooplankton grazing when the functional response of grazers may be nonlinear. Marine Ecology Progress Series 80:285–290.

Evans, G. T., and J. S. Parslow. 1985. A model of annual plankton cycles. Biological Oceanography 3:327–347.

Garver, S. A., and D. A. Siegel. 1997. Inherent optical property inversion of ocean color spectra and its biogeochemical interpretation: I. Time series from the Sargasso Sea. Journal of Geophysical Research 102:18607–18625.

Gran, H. H., and T. Braarud. 1935. A quantitative study on the phytoplankton of the Bay of Fundy and the Gulf of Maine (including observations on hydrography, chemistry and morbidity). Journal Biology Board Canada 1:219–467.

Halldal, P. 1953. Phytoplankton investigations from the weather ship M in the Norwegian Sea. Hvalråd Skr 38:1–91.

Hátún, H., A. B. Sandø, H. Drange, B. Hansen, and H. Valdimarsson. 2005. Influence of the Atlantic subpolar gyre on the thermohaline circulation. Science 309:1841–1844.

Heimdal, B. R. 1974. Composition and abundance of phytoplankton in the Ullsfjord area, North Norway. Astarte 7: 17–42.

Henson, S. A., J. P. Dunne, and J. L. Sarmiento. 2008. Decadal variability in North Atlantic phytoplankton blooms. Journal of Geophysical Research 114(c4):C04013.

Huot, Y., M. Babin, F. Bruyant, C. Grob, M. S. Twardowski, and H. Claustre. 2007. Relationship between photosynthetic parameters and different proxies of phytoplankton biomass in the subtropical ocean. Biogeoscience 4:853–868.

Jackson, G. A. 2005. Coagulation theory and models of oceanic plankton aggregation. Pages 271–292 in I. Droppo, G. Leppard, S. Liss, and T. Milligan, editors. Flocculation in natural and engineered environments. CRC Press, Boca Raton, Florida, USA.

Körtzinger, A., U. Send, R. S. Lampitt, S. Hartman, D. W. R. Wallace, J. Karstensen, M. G. Villagarcia, O. Llinás, and M. D. DeGrandpre. 2008. The seasonal pCO_2 cycle at 49° N/ 16.5° W in the northeastern Atlantic Ocean and what it tells

us about biological productivity. Journal of Geophysical Research 113:C04020.

Landry, M. R. 1993. Estimating rates of growth and grazing mortality of phytoplankton by the dilution method. Pages 715–722 in P. F. Kemp, B. F. Sherr, E. B. Sherr, and J. J. Cole, editors. Handbook of methods in aquatic microbial ecology. Lewis Publishers, Boca Raton, Florida, USA.

Landry, M. R., and R. P. Hassett. 1982. Estimating the grazing impact of marine micro-zooplankton. Marine Biology 67: 283–288.

Landry, M. R., J. Kirshtein, and J. Constantinou. 1995. A refined dilution technique for measuring the community grazing impact of microzooplankton, with experimental tests in the central equatorial Pacific. Marine Ecology Progress Series 120:53–63.

Margalef, R., F. Muñoz, and J. Herrera. 1957. Fitoplancton de las costas de Castellón de enero de 1955 a junio de 1956. Investagaciones Pesqueras 7:3–31.

Maritorena, S., D. A. Siegel, and A. R. Peterson. 2002. Optimization of a semianalytical ocean color model for global-scale applications. Applied Optics 41:2705–2714.

Marra, J., and R. T. Barber. 2005. Primary productivity in the Arabian Sea: a synthesis of JGOFS data. Progress in Oceanography 65:159–175.

Milutinović, S., M. J. Behrenfeld, J. A. Johannessen, and T. Johannessen. 2009. Sensitivity of remote sensing-derived phytoplankton productivity to mixed layer depth: lessons from the carbon-based productivity model. Global Biogeochemistry Cycles 23:GB4005.

Morel, A. 1991. Light and marine photosynthesis: a spectral model with geochemical and climatological implications. Progress in Oceanography 26:263–306.

Paasche, E. 1960. Phytoplankton distribution in the Norwegian Sea in June, 1954, related to hydrography and compared with primary production data. Fiskeridir Skr Ser Havunders 12: 1–77.

Paasche, E., and A. M. Rom. 1962. On the phytoplankton vegetation of the Norwegian Sea in May 1958. Nytt Magasin for Botanik 9:33–60.

Parsons, T. R., and C. M. Lalli. 1988. Comparative oceanic ecology of the plankton communities of the subarctic Atlantic and Pacific oceans. Oceanography and Marine Biology Annual Review 26:317–359.

Platt, T., D. F. Bird, and S. Sathyendranath. 1991. Critical depth and marine primary production. Proceedings of the Royal Society B 246:205–217.

Ramsfjell, E. 1960. Phytoplankton distribution in the Norwegian Sea in June, 1952 and 1953. Fiskeridir Skr Ser Havunders 12:1–112.

Reynolds, C. S. 2006. The ecology of phytoplankton. Cambridge University Press, Cambridge, UK.

Riley, G. A. 1946. Factors controlling phytoplankton populations on Georges Bank. Journal of Marine Research 6:54–72.

Schei, B. 1974. Phytoplankton investigations in Skjomen, a fjord in North Norway, 1970–1971. Astarte 7:43–59.

Siegel, D. A., S. C. Doney, and J. A. Yoder. 2002a. The North Atlantic spring bloom and Sverdrup's critical depth hypothesis. Science 296:730–733.

Siegel, D. A., et al. 2002b. Global distribution and dynamics of colored dissolved and detrital organic materials, Journal of Geophysical Research 107:3228.

Siegel, D. A., S. Maritorena, N. B. Nelson, and M. J. Behrenfeld. 2005. Independence and interdependences among global ocean color properties: reassessing the bio-optical assumption. Journal of Geophysical Research 110:C07011.

Smetacek, V., and U. Passow. 1990. Spring bloom initiation and Sverdrup's critical-depth model. Limnology and Oceanography 35:228–234.

Steemann Nielsen, E. 1957. The general background of oceanic productivity. Pages 91–120 in E. Steemann Nielsen and E. A. Jensen, editors. Primary oceanic production. The autotrophic production of organic matter in the ocean. Galathea Report 1:43–136.

Sverdrup, H. U. 1953. On conditions for the vernal blooming of phytoplankton. Journal du Conseil International pour l'Exploration de la Mer 18:287–295.

Townsend, D. W., M. D. Keller, M. E. Sieracki, and S. G. Ackleson. 1992. Spring phytoplankton blooms in the absence of vertical water column stratification. Nature 360:59–62.

Ward, B. A., and J. J. Waniek. 2007. Phytoplankton growth conditions during autumn and winter in the Irminger Sea, North Atlantic. Marine Ecology Progress Series 334:47–61.

Westberry, T., M. J. Behrenfeld, D. A. Siegel, and E. Boss. 2008. Carbon-based primary productivity modeling with vertically resolved photoacclimation. Global Biogeochemical Cycles 22:GB2024.

APPENDIX

Figures showing nine-year records of phytoplankton biomass and Chl$_{sat}$ at eight-day resolution for the 12 North Atlantic bins, mean annual cycles in phytoplankton carbon and Chl$_{sat}$ at eight-day resolution for the 12 North Atlantic bins, and 5° latitude zonal mean values of phytoplankton net specific growth rate during the positive phase of the annual cycle and spring maximum in surface chlorophyll concentration (*Ecological Archives* E091-069-A1).